Phys Chem Minerals (2002) 29: 19–31
DOI 10.1007/s002690100199

ORIGINAL PAPER

R. D. McDonnell · C. J. Spiers · C. J. Peach

Fabrication of dense forsterite–enstatite polycrystals for experimental studies

Received: 19 October 1999 / Accepted: 18 June 2001

Abstract A practical and reliable method for the preparation of fine-grained forsterite and forsterite–enstatite polycrystals, in the system $MgO–SiO_2$, is described. The method employs state-of-the-art techniques from materials science, namely sol-gel synthesis, powder processing and sintering. The resulting dense polycrystalline materials are homogeneously fine-grained (1–2 μm) and uniformly foam-textured. Moreover, they are highly reproducible in composition and microstructure. The enstatite content can be controlled to within ~1%, in the range 0–50%, and densities up to 98% of theoretical density can be achieved. The method thus yields polycrystalline forsterite–enstatite material suitable for a range of geochemical, petrological and geophysical studies.

Keywords Olivine · Pyroxene · Sintering · Sol-gel · Synthesis

Introduction

The physical and chemical properties of forsterite (fo – magnesium orthosilicate, Mg_2SiO_4) and enstatite (en – magnesium metasilicate, $MgSiO_3$), the magnesium end members of the olivine and pyroxene mineral groups, and their Fe-bearing solid solutions, are of well-known scientific and technological interest. The condensation and reaction of forsterite and enstatite in primordial solar nebulae are believed to play an important role in the fractionation of elements prior to planet formation (Grossman 1972; Anders and Ebihara 1982; Ringwood 1989). In addition, both forsterite and enstatite are major components of the Earth's upper mantle and are thus of considerable importance in controlling its seismic properties, rheological behaviour and thermal structure (Ringwood 1969). Moreover, with the discovery of the near-infrared lasing properties of chromium-doped single crystals, there has recently been renewed interest in forsterite in materials science (Petricevic et al. 1988; Garrett et al. 1991).

This paper describes in detail the fabrication of dense forsterite and forsterite-plus-enstatite polycrystals, employing a state-of-the-art materials science approach involving sol-gel synthesis, powder processing and sintering in air. The method developed allows the production of fine-grained (1 to 2 μm), high-purity forsterite and forsterite–enstatite materials with controlled enstatite content and porosities down to ~2%, i.e. densities up to ~98% of theoretical density (TD). To date, materials with enstatite contents ranging between 0 and 50 vol% have been successfully fabricated. In addition, gels up to 100% enstatite composition have been successfully synthesized. Completely independent control of grain size, enstatite content and porosity is not possible. This is due to the fact that densification is achieved by sintering, during which the reduction of porosity is coupled to grain coarsening, which is itself influenced by second phase content.

The synthesis method described was initially developed to produce starting material (cylinders measuring 25 mm in length × 10 mm diameter) for experiments designed to investigate deformation mechanisms in dry and wet peridotitic systems (McDonnell 1997; McDonnell et al. 1999, 2000). The use of natural rocks in such experiments suffers from the drawback that they are chemically complex, may contain additional, unwanted phases (e.g. spinel, serpentine) and have a water content which cannot be independently controlled (Chopra and Paterson 1981, 1984; Jackson et al. 1992). As an alter-

R. D. McDonnell · C. J. Spiers (✉) · C. J. Peach
HPT Laboratory, Faculty of Earth Sciences,
Utrecht University, PO Box 80021,
3508 TA Utrecht, The Netherlands
Tel.: +31-(0)30-2534972; Fax: +31-(0)30-2537725
e-mail: cspiers@geo.uu.nl

Present address:
R. D. McDonnell
Sun Microsystems Nederland BV,
PO Box 1270, 3800 BG Amersfoort, The Netherlands
e-mail: robert.mcdonnell@holland.sun.com
Tel.: +31-(0)33-4515085; Fax: +31-(0)33-4501356

native, polymineralic materials produced from natural mineral separates are sometimes used (Karato et al. 1986). In both cases, however, the mineral compositions may not be at equilibrium with each other, when first brought to the conditions required for experimentation, so that the results may be influenced by reactions or even partial melting. Polycrystalline aggregates produced from natural olivine and/or pyroxene powders have allowed deformation and other geophysical studies to be extended to fine grain sizes (e.g. Schwenn and Goetze 1978; Karato et al. 1986; Tan et al. 1997). However, such methods have a number of disadvantages. Firstly, high densities can only be achieved from natural olivine or pyroxene powders by hot isostatically pressing (HIPing) low-density compacts prior to experimentation (e.g. Hitchings et al. 1989). This greatly complicates and prolongs experimental procedures. Secondly, as the natural compositions used are iron-bearing, control of oxygen fugacity is essential to ensure that the olivine remains within its stability field during processing. Thirdly, the grinding necessary in powder preparation can lead to chemical contamination and can introduce mechanical damage into the grains. Moreover, the grains produced by grinding are often angular and show a relatively wide grain-size distribution. These features can lead to exaggerated grain growth during HIPing. This limits the minimum achievable grain size to $\sim$10 μm, whereas lower values are desirable, particularly for experimental studies of diffusion creep and the effects of H_2O.

In contrast to natural powder preparation methods, sol-gel techniques have recently been used to produce fine-grained ($\sim$2 μm), Fe-bearing olivine powders, with narrow grain-size distributions, which can be subsequently HIPed to produce dense, polycrystalline aggregates without significant grain growth (Burlitch et al. 1991; Beeman and Kohlstedt 1993). The present approach involves the production of dense fine-grained olivine-orthopyroxene materials in the MgO–SiO_2 system without the need to perform the time-consuming and technically difficult operation of HIPing low-density powders, and without the need to control oxygen fugacity at any stage. The method developed offers a way of preparing reproducible fo–en sample materials with composition 0–50% enstatite, suitable for a wide range of geochemical, petrological and geophysical experiments.

Background on sol-gel processing

Terminology and methods

A brief introduction to sol-gel processing is included here to introduce the necessary materials science terminology and background for the Earth sciences readership. For detailed reviews, the reader is referred to Johnson (1985), Ramsay (1988), Segal (1989) and Hench and West (1990). The key feature of sol-gel methods is that they allow preparation of an intimate mix of reactants which is subsequently reaction-sintered to yield an extremely fine-grained crystalline product. This can then be resintered to form a dense polycrystalline material. Experimental petrologists have long synthesized starting materials via gel routes (Roy and Roy 1954; Roy 1956; Luth and Ingamells 1965; Hamilton and Henderson 1968). More recently, sol-gel processing has attracted major interest in materials science, and the technique is used today for a variety of applications, including the preparation of nuclear fuel, ceramic powders and thin films, bulk glasses, optical fibres and glass ceramics (see Segal 1989 and references therein).

The term sol-gel is an abbreviation for *solution gelation* (Johnson 1985). The *solution* is either (1) a true sol, i.e. a stable suspension of solid colloidal particles in a liquid, or (2) a true solution (liquid phase), e.g. of organometallics such as metal alkoxides $M(OR)_z$, formates $[M(CHOO)_z]$ or acetates $[M(CH_3OO)_z]$ which can react to form solid colloidal particles. Here R represents, for example, the methyl or ethyl functional groups and M represents a metal of valency z. *Gelation* refers to the process of condensation and consolidation of sol particles and/or the reaction of solutions to form condensed solid colloidal particles. Gelation is usually induced by adjusting the solution chemistry. By definition, a sol or solution becomes a gel when the colloid becomes sufficiently consolidated to support stress elastically. At this stage the gel is still wet, consisting of condensed colloidal particles forming a connected network permeated by a residual liquid phase (left from the initial suspension or gelation reactions). Such residual liquids are usually water- or alcohol-based and give rise to the terms *hydrogel* (or *aquagel*) and *alcogel*, respectively. On drying, the gels generally undergo dramatic shrinkage and cracking, resulting in a *xerogel*. By starting with well-mixed solutions, amorphous and chemically homogeneous, multicomponent oxide xerogels can be obtained, achieving mixing of components on the molecular scale. Alternatively, by using multiphase sols or sols mixed with solutions, chemically and structurally *polyphasic* xerogels – or *maximally heterogeneous nanocomposites* (Roy et al. 1986) – can be obtained. The structurally polyphasic (crystalline + amorphous) nature of these nanocomposites, coupled with their chemical heterogeneity on the colloidal scale, controls nucleation, growth (epitaxy) and hence the grain-size distribution of the crystalline phases produced (Komarneni et al. 1987; Roy et al. 1986; Suwa et al. 1986a, b).

Sol-gel processing has several advantages compared with conventional ceramic/mineral synthesis routes such as the use of oxide powders. Firstly, the high surface area and intimate mixing of the colloidal particles results in high reactivity, allowing low-temperature reaction sintering. Secondly, the nanopowders produced have enhanced sinterability compared to coarser powders produced by the reaction of oxides. Thirdly, chemical contamination can be minimized, as little or no comminution is involved. Lastly, the sol-gel process provides a

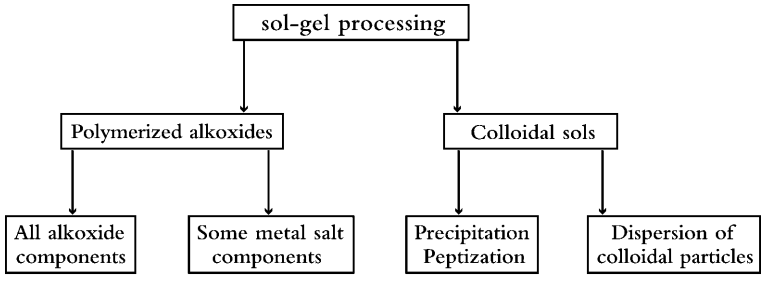

Fig. 1 Classification of sol-gel routes (After Johnson 1985)

means of shaping products using low-temperature casting (e.g. Omatete et al. 1991). The formation of non-equilibrium phases from highly reactive xerogels can be problematic (Edgar 1973). However, this can be overcome by either seeding amorphous monophasic gels with crystalline phases (e.g. Komarneni et al. 1987; Liu et al. 1995) or by using the structurally polyphasic gels as a means of reducing the barrier to nucleation.

Johnson (1985) divides sol-gel processing methods into two broad categories – those using sols of dispersed colloidal particles, and those using alkoxide solutions which hydrolyze and polymerize into gels (Fig. 1). This classification forms a useful subdivision of the major processes involved. However, many workers have developed hybrid methods using both colloidal sols and alkoxide solutions so that, in a sense, such subdivisions are artificial.

Sol-gel processing involving *colloidal sols* (Fig. 1) can follow a number of routes. In the dispersed colloidal sol-gel method, a stable sol is produced by dispersing colloidal particles, with or without the aid of peptization (stabilization of a colloidal suspension by adsorption of electrolytes). In multicomponent systems, the components are mixed as sols (or added to the main sol in solution or as oxide powders) before gelation. Gelation commonly involves the modification of surface charge to reduce repulsive electrostatic forces between the particles and to allow them to coalesce and gel into a continuous network. Thus, gelation in such colloidal systems can be seen as the opposite process to peptization, and sol-gel transitions in such systems are often reversible.

The remaining major class of sol-gel techniques includes routes which also lack a stable sol stage and are truly irreversible in nature. These are the *alkoxide routes* (Fig. 1), in which metal (or semimetal) alkoxides [$M(OR)_z$] are hydrolyzed to form gels directly. This is illustrated in Fig. 2 for the commonly used silicon alkoxide, tetraethyl orthosilicate [TEOS – $Si(OC_2H_5)_4$]. Whilst colloidal methods allow mixing at the colloidal level (10^3 to 10^9 molecules per colloidal particle), alkoxide routes, with cross-condensation of several metal alkoxides, can achieve mixing at the molecular level. Alkoxide routes fall into two main categories, namely all-alkoxide routes and routes where additional components are added as soluble salts. In multicomponent all-alkoxide routes, hydrolysis must be carefully controlled to counteract differing hydrolysis rates of the alkoxides involved, thus avoiding the formation of polymerized clusters of one component (Yoldas 1988).

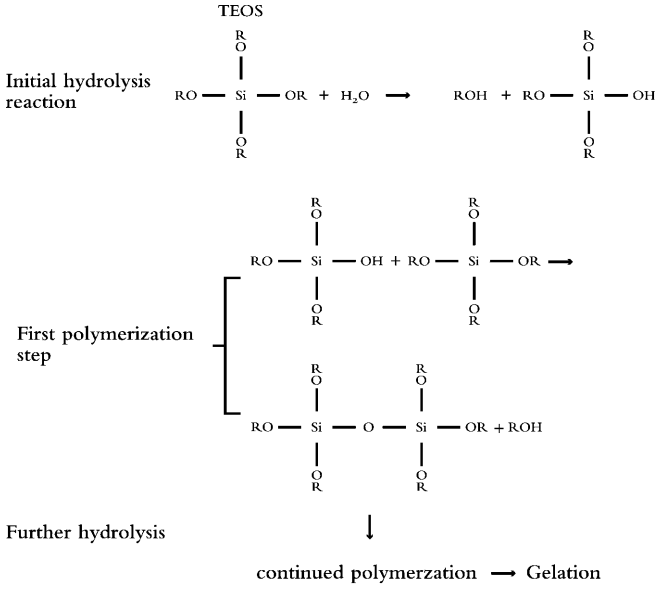

Fig. 2 Schematic representation of the hydrolysis and self-condensation of tetraethylorthosilicate $Si(OC_2H_5)_4$ (TEOS). *R* represents the C_2H_5 group

In the sol-gel processing of silicates, alkoxide routes employing TEOS are the main ones used. When alcohol is used as a solvent, TEOS becomes miscible with water and most aqueous salt solutions (Hamilton and Henderson 1968). However, TEOS is generally slow to hydrolyze and it is therefore common practice to use acid or base catalysts to speed hydrolysis and gelation (Keefer 1984).

Previous work on sol-gel synthesis of forsterite and enstatite

There have been several previous studies directed at the synthesis of forsterite and enstatite powders, and at the production of high-density forsterite polycrystals, using both conventional oxide reactant (Young et al. 1993) and sol-gel routes (Finnerty et al. 1978; Gonczy et al. 1986; De Mott 1987; Beeman 1989; Kazakos et al. 1990; Burlitch et al. 1991; Shiono et al. 1991; Yeager and Burlitch 1991; Echeverria 1992; Hogan et al. 1992; Yeager et al. 1993; Park et al. 1993, 1994a, b; Huang et al. 1994). The main sol-gel-based routes published to date for the production of forsterite and olivine poly-

crystals (Kazakos et al. 1990; Burlitch et al. 1991; Shiono et al. 1991) are outlined below.

Kazakos et al. (1990) described a method for the preparation of forsterite polycrystals by nanocomposite (structurally diphasic), colloidal sol-gel processing (right branch of Fig. 1). In this method, magnesia (MgO) powder with a grain size of 10 nm was added to water, "peptized" with acid (composition and concentration not given), and stirred to produce a "dispersion resembling an opalescent colloidal suspension" (sol). A stoichiometric proportion of colloidal silica sol (Ludox AS40) was then added while stirring continuously. This mixture was subsequently dried at 100 °C and the resulting powder calcined at 400 °C for several hours. Calcination is a high-temperature reaction whereby a solid dissociates to form a gas plus a new solid. The powder product was pellet-pressed to form a so-called greenbody (a shaped/formed but unfired material) and fired at temperatures between 1100 and 1500 °C to form forsterite ceramic.

Burlitch and coworkers (Burlitch et al. 1991; Yeager and Burlitch 1991; Yeager et al. 1993; Park et al. 1993, 1994a, b) have presented an H_2O_2-assisted alkoxide route for the production of forsterite, iron-bearing olivine (Fo_{90}) and chromium-doped forsterite powders. Powders produced by this method were HIPed (1250 °C, 300 MPa, 3 h) by Beeman and Kohlstedt (1993) to produce high-density olivine polycrystals for deformation studies.

Shiono et al. (1991) described a hybrid colloidal/alkoxide method for the preparation of forsterite from TEOS and MgO powder, using ethanol as the solvent. In this procedure, TEOS was first partially hydrolyzed, in the presence of an HCl catalyst. Colloidal MgO powder (10 nm) was then added to the partially hydrolyzed TEOS. The solution was subsequently gelled by the addition of distilled water followed by drying, powder processing and calcination at temperatures in the range 500 to 1500 °C to produce forsterite powder.

Trials using diphasic sol-gel routes

The present investigation, aimed at developing a sol-gel-based process for the fabrication of starting materials for experimental studies, was constrained by the need to produce relatively large quantities of material (> 5 g per sample) combined with a desire to keep the practical procedures as simple and quick as possible. These considerations led to the decision to concentrate on nanocomposite diphasic routes, using the chemically simple $MgO–SiO_2$ system and focusing on colloidal MgO powder and TEOS as starting reagents. These routes are much easier to carry out than the various organometallic routes, including all-alkoxide ones such as that proposed by Burlitch et al. (1991), and are expected to give good microstructural control (Suwa et al. 1986a, b). Accordingly, several attempts were made to reproduce the results described by Kazakos et al. (1990) and Shiono et al. (1991) as detailed below.

Using the method described by Kazakos et al. (1990), dense forsterite polycrystals were successfully produced with grain sizes around 10 μm. However, we found difficulty in obtaining high densities and adequate microstructural and compositional homogeneity. Kazakos et al. (1990) describe their starting suspension, produced by the addition of 10 nm MgO colloidal powder to water, as a magnesia sol. This is misleading, since our trials showed that the colloidal MgO reacts immediately with water to produce a strongly alkaline magnesium hydroxide [brucite – $Mg(OH)_2$] suspension, which gels almost intantaneously on addition of TEOS. Thorough mixing is therefore difficult and may cause the microstructural and compositional heterogeneity which we observed. Adding acid (HCl), following Kazakos et al., did not prevent or improve this behaviour and cannot be considered "peptizing" (as termed by Kazakos et al. 1990), since it simply dissolves the $Mg(OH)_2$ hydration product. Kazakos et al. (1990) present densification curves, which show that the densities of the final ceramic produced from their calcined gels, after pellet-pressing and sintering for 1 h, are almost independent of the sintering temperature between 1200 and 1500 °C. In our trials, with or without acid addition, these results could not be reproduced by following the procedure described, and high densities could be achieved only at temperatures of ~1400 °C.

The sol-gel method of Shiono et al. (1991) was attempted by us in a limited series of test runs, but polycrystals made by sintering the powders produced at ~1300 °C for several hours retained unacceptably high porosities (30%). An alternative, hybrid colloidal/alkoxide method was communicated to the authors by Drs. Shiono and Okamoto (Department of Chemistry and Materials Technology, Kyoto Institute of Technology, Japan). Unlike the method published by Shiono et al. (1991), which did not work satisfactorily for us, the method communicated involves the suspension of colloidal MgO powder (10 nm) in ethanol with a small amount of water. TEOS is then added to the mixture and allowed to prehydrolyze, before gelation is achieved by the further addition of distilled water *without using* either an acidic or alkaline catalyst. However, in our trials using this approach, hydrolysis of TEOS was found to be incomplete, leading to loss of silica on drying of the resulting gel. This was confirmed using gas chromatography of distillates produced from the gels after 24 h gelation.

Several important lessons have been learned during the trials of the diphasic sol-gel routes described by Kazakos et al. (1990) and Shiono et al. (1991). These have played an important role in the development of a successful diphasic approach to the preparation of forsterite–enstatite ceramic materials from MgO and TEOS starting materials and are summarized below.

1. Atmospheric water adsorbed by colloidal MgO powder leads to mass increases, which must be accurately corrected for to obtain the desired reactant proportions.

2. Colloidal suspensions of MgO in water become rapidly hydrated to form $Mg(OH)_2$ and cannot be easily stabilized (cf. Kazakos et al. 1990). This hydration (and subsequent dehydration) and poor stability lead to poor microstructural homogeneity in material made using hydrous suspensions.

3. The suspension of MgO in ethanol (following Shiono et al. 1991) removes the problem of hydration. However, the suspensions remain unstable and appear to be somewhat aggregated, showing signs of sedimentation within ~24 h. Nonetheless, this is sufficiently slow not to lead to problems during synthesis.

4. When using the broad approach of Shiono et al. (1991), the addition of an alkaline catalyst such as NH_4OH, standard in sol-gel processing in petrology (Hamilton and Henderson 1968), is essential to iniatiate gelation, to ensure complete hydrolysis of the TEOS and to ensure a predictable final composition (SiO_2 content).

5. In constrast to the conclusions drawn by Shiono et al. (1991), the heat released from the exothermic forsterite-forming reaction during reaction sintering does not appear to lead to excessive sintering and aggregation of the precursor.

6. Regardless of the sol-gel method used, effective disaggregation of the reaction-sintered precursor and the use of an organic binder such as polyethylene glycol during greenbody formation is essential to the formation of a microstructurally homogeneous product. Comparisons made between polycrystals produced with and without the binder have clearly shown that it plays an important role in the production of a homogeneous greenbody. Polycrystals produced without binder were found to have higher porosities and contained occasional large, high-coordination pores which presumably resulted from uneven packing of the precursor. No residue from the binder was observed in the final product, either macroscopically or using SEM and TEM techniques. Polycrystals produced without sufficient disaggregation of the precursor by sieving were found to have a "measles" texture (Burke 1996) resulting from uneven densification of the powder due to the presence of aggregated particles.

7. Claims that enstatite always forms as a by-product during attempts to make pure forsterite by diphasic sol-gel routes (due to the slow kinetics of solid-state diffusion – see Brindley and Hayami 1965) are likely to be incorrect (cf. Kazakos et al. 1990; Hogan et al. 1992; Park et al. 1994b). It is our view that the presence of enstatite results from the difficulty in controlling the bulk chemistry, caused by a failure to allow for the water content of the MgO reagent (see 2 above), and from uneven distribution of reactants in the gels.

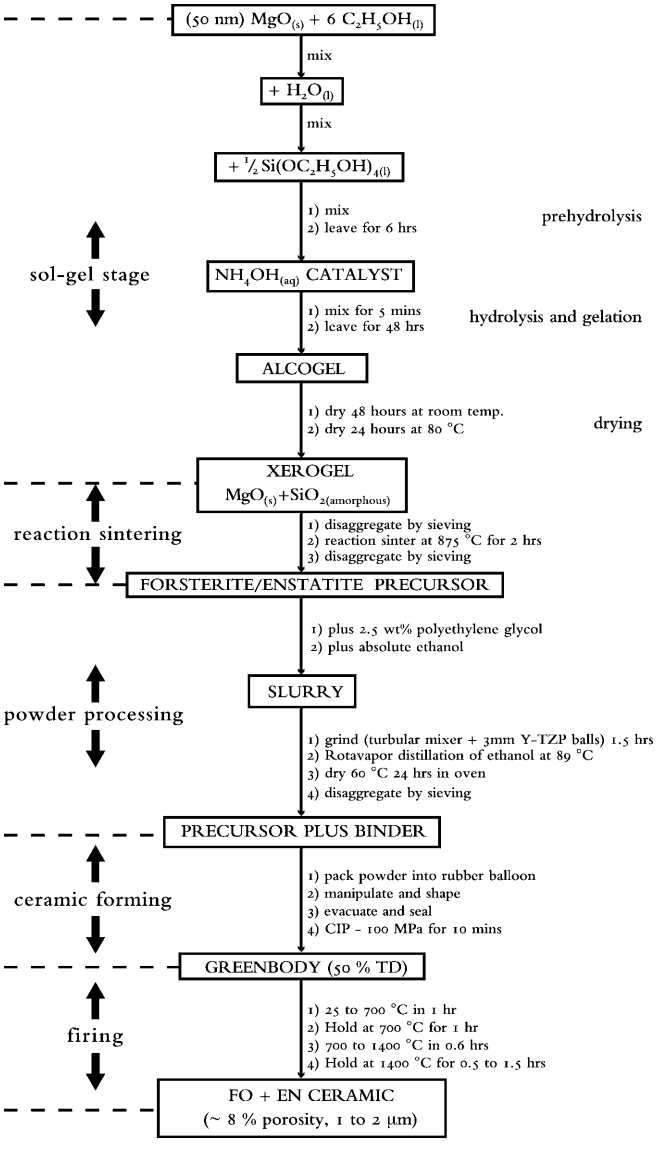

Fig. 3 Flow diagram of the current sol-gel-based fabrication method

Final methodology

The fabrication process finally developed from the numerous trial experiments is founded on a hybrid, sol/alkoxide, sol-gel step, which produces a maximally heterogeneous, chemically and structurally diphasic gel. The process can be subdivided into several stages, namely the sol-gel stage, reaction sintering, powder processing, ceramic forming, firing and machining (see Figs. 3 and 4). These stages will now be described along with the reagents used and the quantities required. In view of frustrations encountered while following previously described methods, the present method is described in detail, in the hope that the reader will be able to fully reproduce the materials made by us in Utrecht.

Reagents and reagent proportions

The following reagents are required:

1. High-purity 50 nm MgO powder (Type 500 A, UBE Industries Japan)
2. Tetraethyl orthosilicate (TEOS. 98%; Merck)
3. Absolute ethanol (Merck)
4. Concentrated NH_4OH (28–30%, Aldrich 22-122-8), diluted by making 50 ml up to 500 ml (pH = 12.32)
5. Polyethylene glycol (MW 8000, Aldrich)

Fig. 4 Photographs of products obtained at various stages during fabrication. *From left to right* CIPed greenbodies, fired material and machined samples (10 mm in diameter by 25 mm in length)

Note that care should be taken to avoid skin contact with, and inhalation of, the reagents.

The reagent proportions required to obtain a forsterite/enstatite volume ratio follow from the relevant synthesis reaction. This is given

$$n\mathrm{MgO}_{(s)} + \mathrm{SiO}_{2(s)} \rightarrow (n-1)\mathrm{Mg_2SiO_{4(s)}} + (2-n)\mathrm{MgSiO_{3(s)}} \qquad (1)$$

where n is the molar ratio of MgO to SiO_2 defined by the choice of reagent proportions. To obtain forsterite plus enstatite ceramics, n must be >1 and <2. If $n > 2$, the stable high temperature assemblage at 1 atmosphere pressure is periclase (MgO) plus forsterite. If $n < 1$, enstatite plus an SiO_2 polymorph are the stable phases. The volume percentage enstatite obtained when $1 \leq n \leq 2$ is given

$$\text{vol\% en} = [100 \cdot (2-n) \cdot V_{\text{en}}]/[(2-n) \cdot V_{\text{en}} + (n-1) \cdot V_{\text{fo}}] \qquad (2)$$

where V_{en} is the molar volume of enstatite (31.31 $\text{cm}^3\ \text{mol}^{-1}$) and V_{fo} is the molar volume of forsterite (43.79 $\text{cm}^3\ \text{mol}^{-1}$). Another useful equation for calculating the volume percentage of enstatite present in a forsterite–enstatite material can be derived by neglecting the small density difference between the two phases ($\rho_{\text{fo}} \sim 3.21$ and $\rho_{\text{en}} \sim 3.20$ g cm^{-3}). This is given

$$\text{vol\% en} = 100 - 100 \cdot [(\text{wt\%MgO} - 40.148)/17.145] \qquad (3)$$

and is valid for the range $40.148 \leq \text{wt\% MgO} \leq 57.293$. It implies that within this range, a change of $\sim$0.171 wt% in MgO content shifts the composition by $\sim$1 vol% enstatite.

In the present procedure, in which TEOS is completely hydrolyzed by the use of $NH_4OH_{(aq)}$ catalyst, there are two main causes for gels departing from the desired composition: (1) the presence of adsorbed water or partial hydration products in the MgO powder, and (2) the evaporation of TEOS during the synthesis procedure. In general, a shortfall in MgO will push the bulk composition towards enstatite. In contrast, any shortfall in SiO_2 pushes the composition towards forsterite which, when a pure forsterite composition is required, can lead to an excess of MgO. In order to correct for these small shifts in composition, the reagents and the procedures used were tested for their true yields in terms of the MgO and SiO_2 components required (see Holloway and Wood 1988, p.178). We have found that a yield of 97.5 wt% for the MgO and 98.0 wt% for TEOS can be used to realistically and accurately correct for the above effects. We caution that these values may need to be modified for local climatic conditions. The quantities of distilled H_2O and absolute ethanol required during the sol-gel stage were calculated using the molar ratios with respect to true MgO yield as indicated in Fig. 3. The volume (in ml) of diluted $NH_4OH_{(aq)}$ catalyst required was scaled with respect to the other reagents using a factor of $54 \times$ mol MgO, as trials indicated that this was sufficient to initiate rapid gelling [i.e. if 1 mol of MgO is used, 54 ml of diluted $NH_4OH_{(aq)}$ is required].

Sol-gel stage

In preparing an individual gel batch, a clean, dry, 1-l polypropylene bottle containing a PTFE-coated magnetic stirrer is weighed along with its lid. Approximately 50 g ($\sim$1.24 mol) of MgO powder is then transferred to the bottle directly from the manufacturer's bag via an inserted tube. The transferred powder is then weighed along with the bottle, lid and magnetic stirrer. The quantities of the other reagents necessary for the synthesis are then calculated accordingly, and the volumes of absolute ethanol (6 mol ethanol to 1 mol MgO) and doubly distilled water (1 mol H_2O to 1 mol MgO) required are measured out into respective measuring cylinders. The ethanol is decanted carefully into the bottle containing the MgO powder, so as not to displace powder from the bottle. The bottle is then capped and the mixture stirred for $\sim$5 min, using the magnetic stirrer, until the powder becomes homogeneously dispersed in the ethanol. The distilled water is then added to the bottle from the measuring cylinder and the bottle recapped, while the suspension is stirred continuously. After approximately half an hour, the appropriate amount of TEOS (i.e. appropriate for a given composition and allowing for the yield factor) is weighed into a measuring cylinder and added to the MgO suspension while stirring continuously; the measuring cylinder must be carefully rinsed several times with ethanol to wash out all the TEOS. The mixture is then left for 6 h with occasional stirring. Thereafter, the dilute NH_4OH solution is added to initiate gelation. The bottle is then closed and stirred for approximately 5 min and the mixture, smelling strongly of ammonia, is now left undisturbed to allow gelation to take place.

Within approximately 1 h, a rigid, homogeneous alcogel will form. This should be left undisturbed for $\sim$48 h to ensure that hydrolysis of the TEOS is complete. This alcogel is subsequently scraped from the bottle into a clean, glazed, flat ceramic bowl and spread evenly to increase its exposed surface area. The bowl plus alcogel is then placed in a fume cupboard to dry at room temperature for 48 h. The resulting xerogel must then be gently ground in the bowl and left for several hours in a fume cupboard before drying at 80 °C for 24 h. Note that great care has to be taken to ensure that the gel is fully dry, as any residual ethanol can lead to combustion of the gel during reaction sintering. The dried xerogel is finally disaggregated by forcing it through a nylon sieve (0.5×0.5-mm mesh size) with the aid of a plastic spatula.

Reaction sintering

The dried and disaggregated xerogel is next placed in high-density, 100% alumina crucibles and reaction sintered at 875 °C for 2 h in a laboratory furnace with molybdenum disilicide elements (Naber LHT16/R). A heating rate of approximately 14 °C min^{-1} is used to reach this reaction-sintering temperature. The resulting forsterite–enstatite precursor is allowed to cool to room temperature in the furnace over several hours, before being disaggregated by forcing it twice through a nylon sieve. The term precursor is used here as the material at this point is not yet fully reacted to forsterite plus enstatite ($\sim$70% reacted at this stage).

Powder processing

The disaggregated precursor is next placed in a 1-l polypropylene bottle along with 2.5 wt% polyethylene glycol binder (crystalline solid) and sufficient absolute ethanol ($\sim$500 ml) to produce a liquid slurry. The bottle is filled $\sim$3/4 full with $\sim$3 kg of 3 mm diameter Yttria stabilized zirconia (Y-TZP) grinding balls (Ceratec Technical Ceramics), and securely capped before being placed in a turbular mixer for 1.5 h. After grinding, the slurry is decanted into a rotavapor dryer flask, using a ceramic filter funnel to capture the grinding balls (no filter paper required). Slurry remaining on the grinding balls is then rinsed into the flask using absolute ethanol

from a wash bottle. The ethanol is then distilled off using a rotavapor dryer at ~89 °C, and the resulting soft cake of forsterite/enstatite precursor plus polyethylene glycol binder removed from the rotavapor flask and placed in a drying oven at 60 °C for ~24 h. After drying, the cake is gently broken up, using a glazed ceramic mortar and pestle, before returning to the drying oven at 60 °C. Once fully dry, the powder is disaggregated once again by forcing it through a nylon sieve.

Ceramic forming

To form appropriately sized greenbodies, individual 15-g batches of the polyethylene-glycol-bonded forsterite/enstatite precursor are weighed out and transferred to small latex balloons (10 × 1.5 cm – non-inflated dimensions). The open end of each balloon is sealed by the insertion of a 15-cm-long steel evacuation tube (6.3 mm OD, 1 mm ID), tipped with a cotton fabric filter, against which the balloon neck formed a tight, powder-free closure.

After insertion of the evacuation pipe, the powder must be manually manipulated for several minutes in order to further disaggregate the powder until it has a smooth, well-lubricated, free-flowing aggregate-free feel. The powder is then shaped into a crude cylinder, ~4.5 cm long and ~2.0 cm in diameter, and a vacuum (~1 Torr) applied using a standard laboratory vacuum pump. The powder-filled balloon is again manipulated and rolled at this stage to help the air escape and to facilitate closer packing of the grains. As the air is removed, the powder becomes stiff and further shaping is difficult. The balloon is then evacuated for a further 5 min before carefully removing the evacuation tube, without allowing air back into the balloon. The balloon is subsequently tied at the neck and placed in a condom, which is also evacuated and tied. When 10 to 15 samples have been prepared in this way, they are transferred to an oil-medium pressure vessel for cold isostatic pressing (CIP). This is conducted at 100 MPa for 10 min at room temperature. The samples – now greenbodies – are retrieved and the rubber jackets removed (Fig. 4).

Firing and machining

Firing is carried out using a programmable laboratory furnace. The greenbodies produced by CIPing are wrapped together in platinum foil. The exact sintering temperature and duration required are predetermined from a series of batch-specific test runs. This procedure is necessary in order to allow for small differences in greenbody structure and composition between sample batches. Following this approach, final porosities in the range 2 to 30% can be achieved as desired. The furnace heating cycle is controlled using the builtin programmable PID controller and consisted of five steps:

1. Linear heating from room temperature to 700 °C in 1 h (~11.25 °C min^{-1}). This gradual heating of the sample allows loss of volatiles and binder (polyethylene glycol) burnout.
2. Constant temperature heat treatment at 700 °C for 1 h to fully ensure that binder burnout to goes to completion.
3. Linear heating from 700 °C to the sintering temperature (e.g. 1400 °C), in 36 min (19.44 °C min^{-1}). This rapid heating stage allows the greenbody to reach the sintering temperature whilst undergoing the minimum of microstructural evolution.
4. Constant temperature heat treatment at the firing temperature (at 1400 to 1450 °C) for ~30 min to yield 8% porosity and 3 to 4 h to yield ~2% porosity.
5. Uncontrolled cooling to room temperature, achieved by simply switching off the furnace. Note that the furnace buffers the temperature drop sufficiently to prevent damage by thermal shock (initial cooling rate ~7 °C min^{-1}, slowing to ~4 °C min^{-1} at ~1000 °C).

After firing, the hard, white forsterite-plus-enstatite billets are easily machined using water-cooled diamond tools (Fig. 4).

Process progress and material characterization

In the following, thermal analysis results and other data will be presented in relation to selected aspects of the fabrication process. We present data on the properties and structure of processed material at various intermediate stages and on the compositional and microstructural characteristics of the final polycrystalline forsterite/enstatite product. Given the large number of process variables, it has not been possible to fully investigate all aspects of this multistage process.

Xerogel and the reaction-sintered precursor

Powder X-ray diffraction (XRD) analysis was performed on the xerogel before reaction sintering, using a Philips PW-1700 XRD instrument. This proved the xerogel to be structurally diphasic, by virtue of the fact that MgO is the only crystalline phase present so that the silica component must be present in amorphous form (see Figs. 5 and 6a). Differential thermal analysis (DTA) of the xerogel, illustrated in Fig. 7, shows a sharp exothermic peak at 880 °C, corresponding to the forsterite-forming reaction. XRD of the reaction sintered

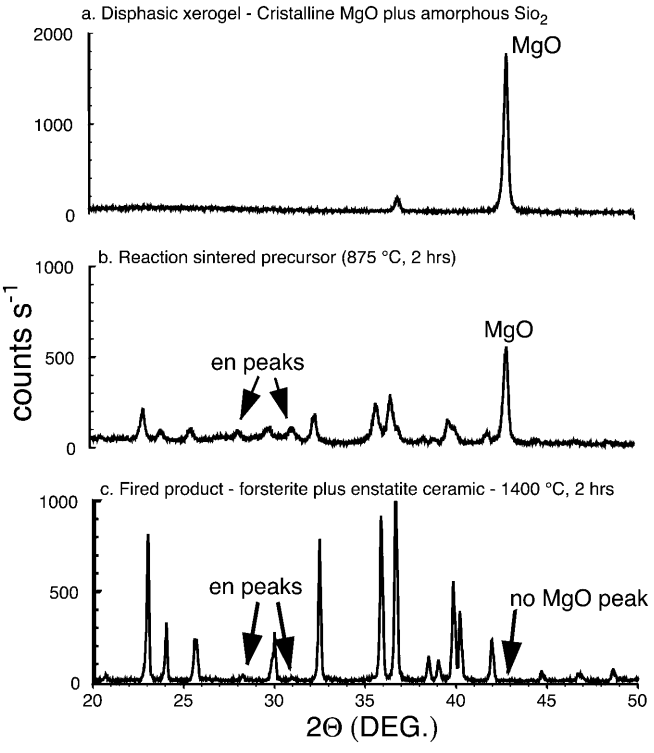

Fig. 5a–c Powder X-ray diffractograms obtained at various stages of processing. **a** The dried xerogel showing that the only crystalline phase present is MgO. Note that the small peak present is the MgO {1 1 1} reflection. **b** The reaction-sintered precursor showing forsterite and enstatite peaks, with remaining MgO indicating that the reaction has not gone to completion. **c** The final material with only forsterite and enstatite peaks present

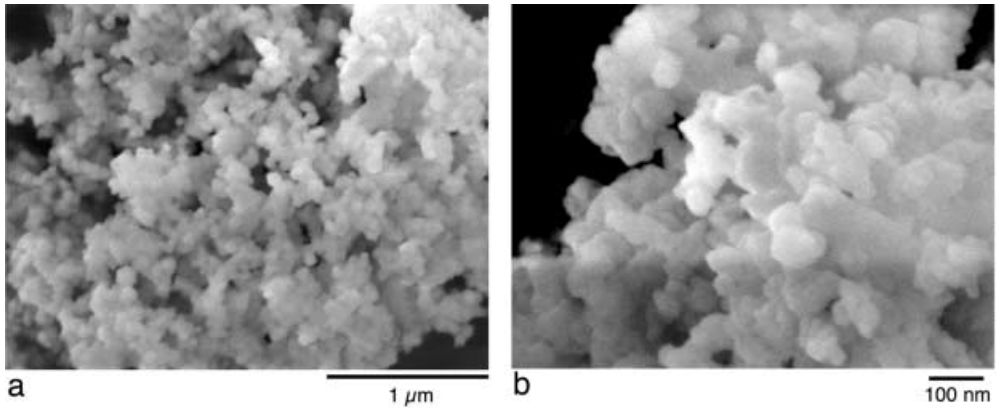

Fig. 6a, b High-resolution scanning electron microscopy (HR–SEM) of gels. **a** The xerogel. **b** Reaction-sintered forsterite–enstatite precursor

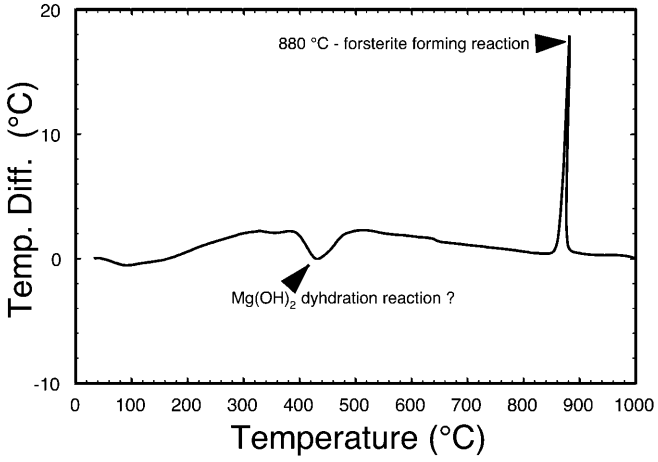

Fig. 7 Differential thermal analysis (DTA) of xerogel produced by the current method. Note the exothermic reaction peak at ~880 °C corresponding to the formation of forsterite (cf. Shiono et al. 1991). Curve obtained using a heating rate of 10 °C min^{-1}

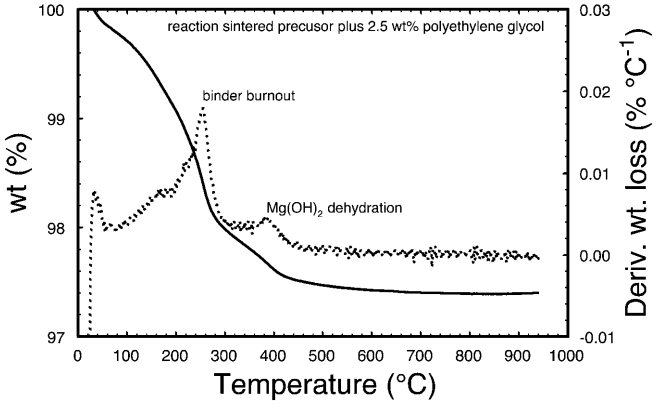

Fig. 8 Thermogravimetric analysis (TGA) of reaction-sintered precursor with ~2.5 wt% polyethylene glycol binder added. Note binder burnout peak at ~260 °C. The *solid line* is the percentage weight loss with temperature. The *dotted line* is the derivative of weight loss. Data obtained using a TA Instruments TGA 2950 analyzer with heating at 50 °C min^{-1}

precursor (2 h at 875 °C) shows that much of the gel has reacted to forsterite at this stage (Fig. 5). However, MgO reflections were still present and indicate that the reaction had not gone to completion. High-resolution scanning electron microscopy (HR-SEM) of the reaction-sintered precursor showed that the average grain size was ~50 to 100 nm (Fig. 6b).

Binder burnout and firing stage (sintering) behaviour

Thermogravimetric analysis (TGA) of the greenbodies containing polyethylene glycol binder has shown that binder burnout starts at ~250 °C and that weight loss continues up to 550 °C (Fig. 8). The densification behaviour of 5 and 10 vol% enstatite plus forsterite polycrystals after binder burnout, with initial porosity of ~50%, have been systematically investigated by means of batch heat treatment experiments conducted at temperatures in the range 1300–1500 °C. The density and grain size of the materials was measured as a function of time by extracting samples at appropriate intervals (see Fig. 9a, b and c). Densities were determined using a modified Archimedes method (Morrel 1985). Grain size was measured using computer-based image analysis to determine grain areas from grain-boundary tracings. The material studied exhibited increased rates of densification with increasing temperature, with the majority of densification (to porosities in the range 4 to 2%) occurring in the first 1 to 5 h. Samples fired at temperatures >1475 °C showed extremely rapid densification followed by abnormal (discontinuous) grain growth. SEM study showed evidence of melt films being developed within grain boundaries in these samples. It is clear from the densification and grain growth curves (Fig. 9a, b and c) that a given composition, firing temperature and firing time result in a specific final porosity and specific grain size, so that it is not possible to independently vary final porosity, grain size and composition. Moreover, reduction of porosity below 2% (without abnormal grain growth and grain boundary melting) clearly requires very long sintering times. Nonetheless, high-density material (2–4% porosity) can be efficiently produced at 1400–1450 °C using firing times of 2–5 h.

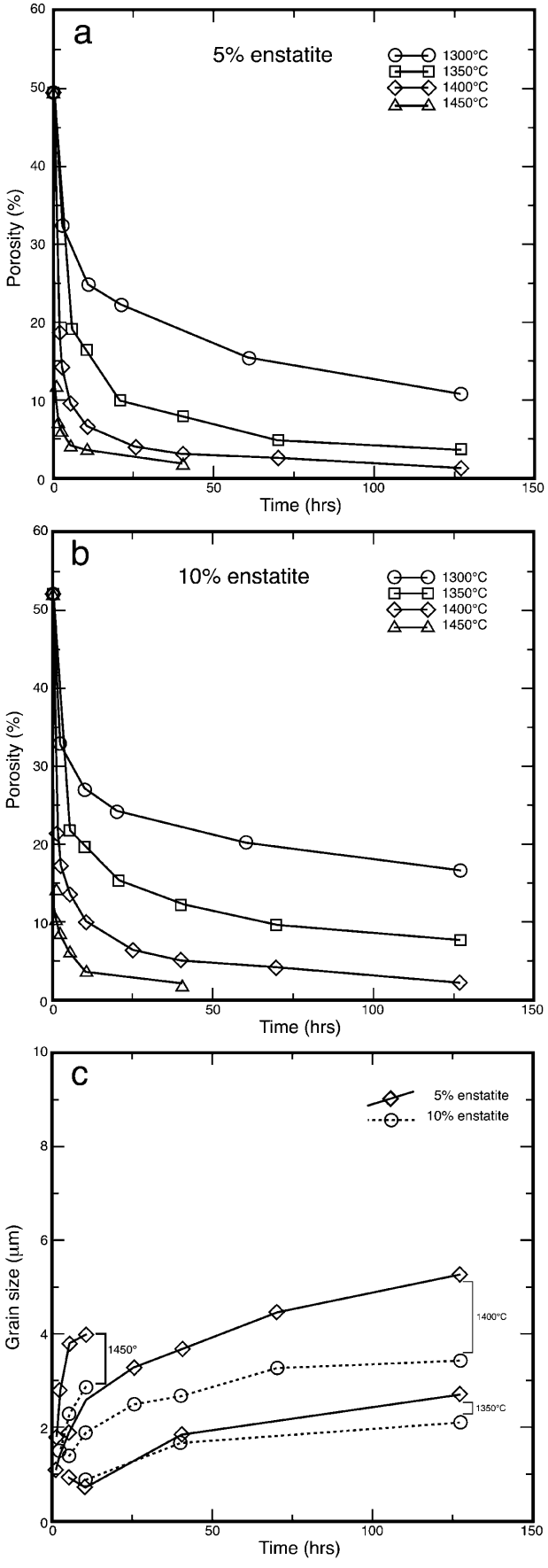

Fig. 9 a, b Densification curves for forsterite plus 5 vol% and 10 vol% enstatite, respectively, prepared using the present method. Porosities determined using the Archimedes method applied to individual samples heat-treated for different times. **c** Final grain size (mean equivalent circular diameter, determined from the measured grain areas) versus sintering time for material with 5 and 10% enstatite

Chemical characterization of the final polycrystal

Phase content

Qualitative and semiquantitative phase analysis of selected final polycrystals was carried out using the aforementioned powder XRD method. Following an approach similar to that described by Cullity (1978), the sensitivity of the technique to the presence of MgO and enstatite phases was accurately calibrated using systematically varied mechanical mixtures (standards) prepared from high-purity MgO (UBE Industries), enstatite (hydrothermal synthesis at 800 MPa and 1000 °C, in house) and forsterite (Cerac B.V.). The calibrations showed that the X-ray diffraction procedure used could detect enstatite contents ≥1 vol% and MgO contents ≥0.5 vol%.

Only forsterite and enstatite peaks could be identified in the final fired materials, indicating that reaction (1) had gone to completion, within the above resolution limits (Fig. 10). Moreover, both the XRD data and fractional area analysis, carried out on images obtained using transmission electron microscopy (TEM), yielded enstatite contents in agreement with the starting, yield-corrected gel compositions. On this basis, it was inferred that the reagent proportions and yield corrections used give control of enstatite content to within $\sim \pm 1\%$. Note that the enstatite phase in the final material and calibration samples was probably proto-enstatite, according to detailed, but as yet unpublished, electron diffraction studies carried out in the TEM at Bayreuth by T. Flierevoet (personal communication). Samples designed by reactant proportions to have final enstatite contents of 0, 2.5, 5.0, 10, 15, 20 and 50% have been successfully prepared, with both XRD and TEM image analysis confirming the final enstatite content (Fig. 10).

In addition to identification of the crystalline phases using XRD, conventional TEM observations have shown that polycrystals produced at temperatures up to 1450 °C, with the full range of enstatite contents of 0–50 vol%, are free from detectable melts. However, high-resolution TEM has not yet been attempted. Accordingly, the presence of melt films or blebs at the corresponding scale (≤2 nm) cannot be discounted.

Bulk chemistry

A preliminary investigation of the bulk chemistry of final polycrystals with 2.5 vol% enstatite has been carried out, using both electron probe microanalysis (EPMA)

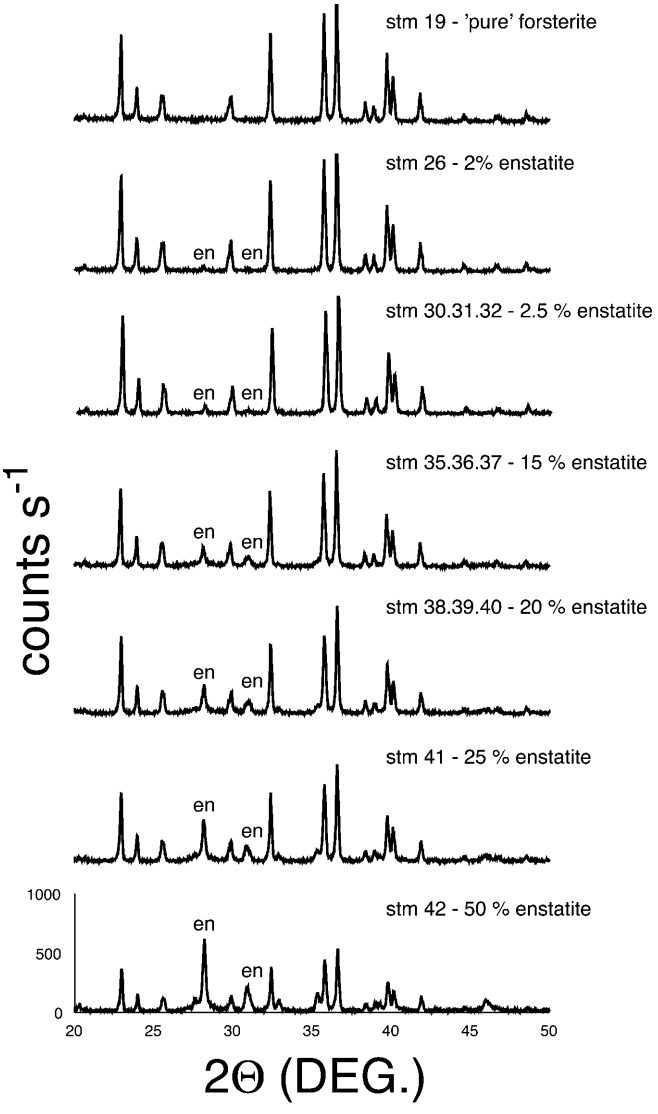

Fig. 10 Powder X-ray diffractograms (XRD) for final products with enstatite contents up to ~50%. NB The absence of MgO in all these samples indicates complete reaction of the reagents

and inductively coupled plasma atomic emission spectroscopy (ICP–AES), to determine the level of contamination during processing. EPMA was carried out using a JEOL superprobe using four wavelength-dispersive spectrometers (WDS) set up for the elements Al, Ca, Na, K, Fe, Co, Ni, Mo, Y and Zr, as these are among the most likely contaminants from grinding media, crucibles, furnace-heating elements and so on. The beam was defocused to a width of ~10 μm, so that the analyses obtained were effectively bulk analyses, sampling 20 to 100 grains and the intervening grain boundaries. The ICP–AES was used to measure the concentrations of a suite of elements including all those analyzed using EPMA. Allowing for contamination of the probe samples by alumina during polishing, both the EPMA and ICP–AES results indicated that all elements investigated were below the detection limits of the techniques used, i.e.~0.02 wt% and ~10 ppm, respectively.

Microstructure of the final ceramic

Microstructural observations of final polycrystals with 2.5 vol% enstatite were made using a Philips XL30 field emission gun (FEG) scanning electron microscope (SEM), operating at 20 kV and 70° tilt in orientation contrast mode. Using this technique, un-etched, uncoated, Syton (colloidal silica)-polished samples could be examined, the contrast between grains resulting from differences in crystallographic orientation. This method yielded better results than etching followed by conventional SEM imaging, as the detailed pore and grain boundary microstructure remained relatively uncorrupted using our approach.

The final polycrystals are microstructurally homogeneous. The typical microstructure obtained is illustrated in Fig. 11, for material with 2.5 vol% enstatite fired at 1400 °C for 1 h (~8% porosity, Fig. 11a, b) and 3 h (~3% porosity, Fig. 11c, d). The grains show a foam texture and have a narrow grain-size distribution with grain sizes typically between 1 and 2 μm. Grain boundaries are straight or gently curved and equilibrium triple junctions of 120° are common. Both intragranular and intergranular pores are present. The bulk of the total porosity is made up of intergranular pores located between two to six grain neighbours and ranging between one half to one tenth of the average grain diameter in size. Where intergranular pores intersect grain boundaries they are characterized by dihedral angles $> 60°$. These pores appear rounded and disconnected in two-dimensional cross-section. No melts or other grain-boundary phases have been observed using the SEM. Figure 11e shows the microstructure obtained after hot isostatic pressing (HIPing), of air-fired material, in the presence of water (0.5 wt% H_2O) at 950 °C and 600 MPa for 24 h. This hot-pressed material possessed an initial pre-HIPing porosity of ~8%, which decreased to ~2% during HIPing. Clearly, the residual 2% porosity is mainly intragranular and therefore very difficult to eliminate.

Quantitative grain-size analysis has been carried out on a number of the standard air-fired samples with 2.5 and 5% enstatite, using computer-based image analysis. Grain-size analysis data show that the final materials always have a narrow grain-size distribution (Fig. 12), with the measured equivalent circular diameters (ECDs) of ~60% of the grains falling in a 1-μm interval around a mean value of ~1.3 μm. The measured grain-size distributions are approximately log-normal, which is consistent with previous studies of grain-size distributions resulting from normal grain growth (Hillert 1965; Mendelson 1969). Recall that grain-growth data are presented in Fig. 9c.

Discussion and conclusions

In the present study, structurally diphasic, sol-gel routes to fine-grained forsterite powders developed by previous

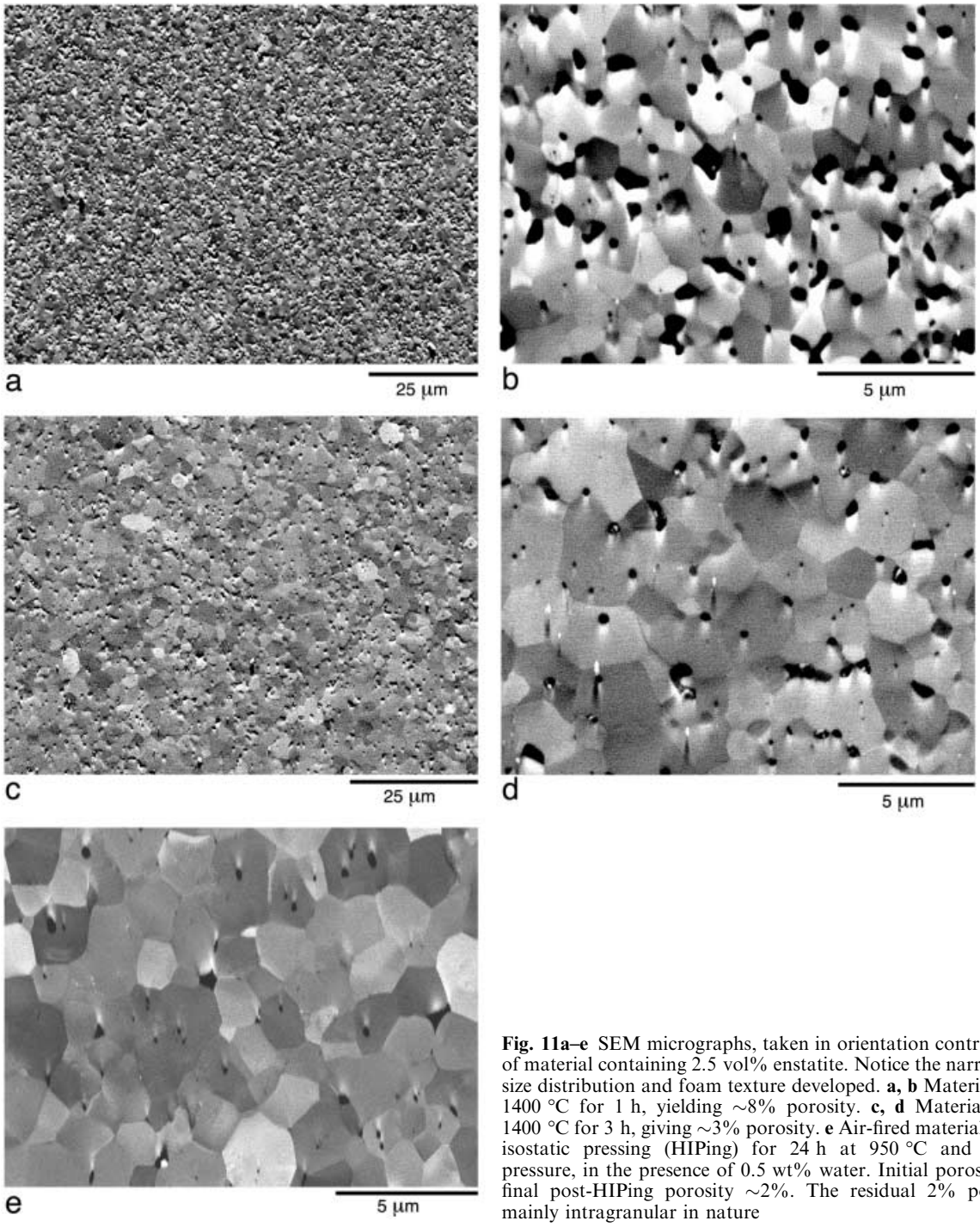

Fig. 11a–e SEM micrographs, taken in orientation contrast mode, of material containing 2.5 vol% enstatite. Notice the narrow grain-size distribution and foam texture developed. **a, b** Material fired at 1400 °C for 1 h, yielding ~8% porosity. **c, d** Material fired at 1400 °C for 3 h, giving ~3% porosity. **e** Air-fired material after hot isostatic pressing (HIPing) for 24 h at 950 °C and 600 Mpa pressure, in the presence of 0.5 wt% water. Initial porosity ~8%; final post-HIPing porosity ~2%. The residual 2% porosity is mainly intragranular in nature

workers have been tested. From this starting point, a practical and reliable sol/alkoxide method has been developed for reproducible manufacture of dense, fine-grained (1–2 μm) forsterite and forsterite–enstatite polycrystals, with controlled enstatite content in the range 0–50% and densities up to 98% of theoretical density. During sintering of the reacted ceramic powders, normal grain growth is accompanied by porosity reduction, and it is this that allows the high densities to be achieved. The coupling of grain growth and densification implies that independent control of grain size and porosity is not possible. However, final porosities (2–50%) can be controlled by careful adjustment of sintering temperature/duration.

Let us now briefly consider the possible reaction mechanism. The work of Roy and coworkers (Roy et al. 1986; Suwa et al. 1986a, b; Komarneni et al. 1987) suggests that epitaxial growth of forsterite on the MgO is probably important in controlling the microstructure of the final material produced from the diphasic gel. The role of solid state epitaxy in the formation of forsterite has not been investigated here. However, the proven

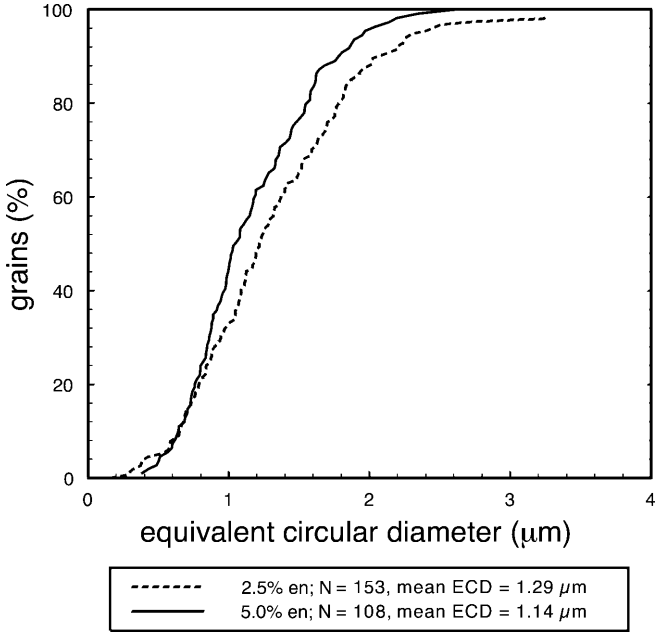

Fig. 12 Grain-size distributions for typical fo–en polycrystals produced by the present method. *Solid line* for material with 5% enstatite fired at 1400 °C for 60 min, final porosity of ~8.5%; *dashed line* for material with 2.5% enstatite fired at 1450 °C for 60 min, final porosity of ~8.8%. Grain size is expressed as an equivalent circular diameter (ECD) which is the diameter of a circle equal in area to the measured grain area. Data obtained from computer-based image analysis of grain-boundary tracings produced from SEM micrographs

diphasic nature of our xerogel implies that it must be composed of highly uniform crystalline MgO grains (derived from the 50 nm powder) coated with amorphous silica. This spatial, chemical and structural makeup is believed to result in highly localized reaction of MgO and SiO_2, leading to an extremely uniform (mono-disperse) forsterite–enstatite precursor. In other words, the uniform microstructure of the final polycrystals is presumed to reflect the original xerogel structure. With regard to the production and persistence of enstatite, reported by other workers in their attempts to make pure forsterite via diphasic sol-gel routes (Kazakos et al. 1990; Hogan et al. 1992; Park et al. 1994b), we believe this to arise from difficulties in controlling the bulk composition of the gel, rather than the slow kinetics of solid-state diffusion-controlled reaction (Brindley and Hayami 1965).

Acknowledgements The work reported here was supported by The Netherlands Organization for Scientific Research (NWO) in the form of research studentship 751-353-026. Dr. R. Terpstra, Dr. J. Gerritsen, H.Gorter and Dr. P. Buining are gratefully acknowledged for their advice on ceramic processing during time spent by R.D. McD. at the Centre for Technical Ceramics (TNO-CTK) in Eindhoven. Dr. T. Shiono and Dr. Y. Okamoto, of the Department of Chemistry and Materials Technology, Kyoto Institute of Technology, are thanked for discussions and advice during development of the current method. P. van Krieken and Martyn Drury are also thanked for assistance and/or advice. An anonymous reviewer made comments which significantly improved the manuscript.

References

Anders E, Ebihara M (1982) Solar-system abundance of the elements. Geochim Cosmochim Acta 46: 2363–2380

Beeman ML (1989) Deformation of olivine-glass aggregates at high temperatures and confining pressures. PhD Thesis Cornell University, Ithaca, NY, pp 118

Beeman ML, Kohlstedt DL (1993) Deformation of fine-grained aggregates of olivine plus melt at high temperatures and pressures. J Geoph Res 98(B4): 6443–6452

Brindley GW, Hayami R (1965) Kinetics and mechanism of formation of forsterite (Mg_2SiO_4) by solid state reaction of MgO and SiO_2. Philos Mag 12: 505–514

Burke JE (1996) Lucalox (TM) Alumina: the ceramic that revolutionized outdoor lighting. MRS Bulletin 21(6): 61–68

Burlitch JM, Beeman ML, Riley BB, Kohlstedt DL (1991) Low-temperature synthesis of olivine and forsterite facilitated by hydrogen peroxide. Chem Mater 3: 692–698

Chopra PN, Paterson MS (1981) The experimental deformation of dunite. Tectonophysics 78: 453–473

Chopra PN, Paterson MS (1984) The role of water in the deformation of dunite. J Geoph Res 89(B9): 7861–7876

Cullity BD (1978) Elements of X-ray diffraction, 2nd edn. Addison-Wesley, Reading, Massachusetts, pp 555

De Mott GJ (1987) Preparation of fayalite by solution-precipitation methods. MSc Thesis Cornell University, NY University

Echeverria LM (1992) Enstatite ceramics: a multicomponent system via sol-gel. J Non-Cryst Sol 147 148: 559–564

Edgar AD (1973) Experimental petrology – Basic principles and techniques. Clarendon Press, Oxford, pp 217

Finnerty TA, Waychunas GA, Thomas WM (1978) The preparation of starting mixes for mineral syntheses by a freeze-dry technique. Am Mineral 63: 415–418

Garrett MH, Chan VH, Jessen HP, Whitmore MH, Sacra A, Singel DJ, Simkin DJ (1991) Comparision of chromium-doped forsterite and akermanite laser host crystals. Opt Soc Am Proc Adv Solid-State Lasers 10: 76–80

Gonczy ST, Lawson RJ, Rosen BI (1986) Preparation of ceramics. In: US Patent No. 4608215

Grossman L (1972) Condensation in the primative solar nebula. Geochim Cosmochim Acta 36: 597–619

Hamilton DL, Henderson CMB (1968) The preparation of silicate compositions by a gelling method. Min Mag 36: 832–838

Hench LL, West JK (1990) The sol-gel process. Chem Rev 90: 33–72

Hillert M (1965) On the theory of normal and abnormal grain growth. Acta Metallogr 13: 227–238

Hitchings RS, Paterson MS, Bitmead J (1989) Effects of iron and magnetite additions in olivine-pyroxene rheology. Phys Earth Planet Inter 55: 277–291

Hogan ME, Martin E, Ober CK, Hubbard CR, Porter WD, Cavin OB (1992) Poly(methacrylate) precursors to forsterite. J Am Ceram Soc 75(7): 1831–1838

Holloway JR, Wood BJ (1988) Simulating the Earth – experimental geochemistry. Unwin Hyman, Boston

Huang CH, Kuo DH, Kim YJ, Kriven WM (1994) Phase stabilty of chemically derived enstatite ($MgSiO_3$) powders. J Am Ceram Soc 77(10): 2625–2631

Jackson I, Paterson MS, FitzGerald JD (1992) Seismic wave dispersion and attenuation in Aheim dunite: an experimental study. Geophys J Int 108: 517–534

Johnson DWJ (1985) Sol-gel processing of ceramics and glass. Am Ceram Soc Bull 64(12): 1597–1602

Karato S-L, Paterson MS, FitzGerald JD (1986) Rheology of synthetic olivine aggregates: influence of grain size and water. J Geophys Res 91(B8): 8151–8176

Kazakos A, Komarneni S, Roy R (1990) Preparation and densification of forsterite (Mg_2SiO_4) by nanocomposite sol-gel processing. Mat Lett 9(10): 405–409

Keefer KD (1984) The effect of hydrolysis conditions on the structure and growth of silicate polymers. Mater Res Soc Sym Proc 32: 15–24

Komarneni S, Suwa Y, Roy R (1987) Enhancing densification of 93% Al_2O_3–7% MgO tri-phasic xerogels with crystalline a-Al_2O_3 and $MgAl_2O_4$ seeds. J Mater Sci Lett 6(5): 525–527

Liu C, Komarneni S, Roy R (1995) Crystallization and seeding effect in $BaAl_2Si_2O_8$ gels. J Am Ceram Soc 78(9): 2521–2526

Luth WC, Ingamells CO (1965) Gel preparation of starting materials for hydrothermal experimentation. Am Mineral 50: 255–258

McDonnell RD (1997) Deformation of fine-grained synthetic peridotite under wet conditions. PhD Thesis Geologica Ultraiectina 152. Utrecht University, pp 195

McDonnell RD, Peach CJ, Spiers CJ (1999) Flow behaviour of fine-grained synthetic dunite in the presence of 0.5 wt% H_2O. J Geophys Res 104(B8): 17823–17845

McDonnell RD, Peach CJ, Van Roermund H, Spiers CJ (2000) Effect of varying enstatite content on the deformation behavior of fine-grained synthetic peridotite under wet conditions. J Geophys Res 105(B6): 13535–13553

Mendelson MI (1969) Average grain size in polycrystalline ceramics. J Am Ceram Soc 52(8): 443–446

Morrell R (1985) Handbook of properties of technical and engineering ceramics, part 1: an introduction for the engineer and designer. Nat Phys Lab HMSO, London

Omatete OO, Janney MA, Strehlow, RA (1991) Gelcasting – a new ceramic-forming process. Am Ceram Soc Bull 70(10): 1641–1649

Park DG, Burlitch JM, Geray RF, Dieckmann R, Barber DB, Pollock CR (1993) Sol-gel synthesis of chromium-doped forsterite. Chem Mater 5: 518–524

Park DG, Duchamp JC, Duncan TM, Burlitch JM (1994a) Preparation of forsterite by pyrolysis of a xerogel: the effect of water. Chem Mater 6: 1990–1995

Park DG, Martin HE, Ober CK, Burlitch JM, Cavin OB, Porter WD, Hubard CR (1994b) Crystallization of precursors to forsterite and chromium-doped forsterite. J Am Ceram Soc 77(1): 33–40

Petricevic V, Gayen SK, Alfano RR, Yamagishi K, Anzai H, Yamaguchi Y (1988) Laser action of chromium-doped forsterite. Appl Phys Lett 52(13): 1040–1042

Ramsay JDF (1988) Characterisation of colloids and gels. Mater Res Soc Symp Proc 121: 293–304

Ringwood AE (1989) Significance of the terrestrial Mg/Si ratio. Earth Planet Sci Lett 95: 1–7

Roy R (1956) Aids in hydrothermal experimentation: II. J Am Ceram Soc 39: 145–146

Roy DM, Roy R (1954) An experimental study of the formation and properties of synthetic serpentines and related layer silicate minerals. Am Mineral 39: 957–975

Roy R, Suwa Y, Komarneni S (1986) Nucleation and epitaxial growth in diphasic (crystalline + amorphous) gels. In: Hench LL, Ulrich DR (eds) Science of ceramic chemical processing. Wiley, New York, pp 234

Schwenn MB, Goetze C (1978) Creep of olivine during hot-pressing. Tectonophysics 48: 41–60

Segal D (1989) Chemical synthesis of advanced ceramic materials (ed. 1991). Chemistry of solid-state materials, vol.1. Cambridge University Press, Cambridge, pp 182

Shiono T, Nishida T, Okamoto Y, Sugishima Y, Nishikawa T (1991) Preparation and characterization of forsterite powder derived from silicon alkoxide and magnesium oxide. Ceramic Trans (Ceram Powder Sci IV) 22: 6

Suwa Y, Komarneni S, Roy R (1986a) Solid-state epitaxy demonstrated by thermal reactions of structurally diphasic xerogels: the system Al_2O_3. J Mat Sci Lett 5: 21–24

Suwa Y, Roy R, Komarneni S (1986b) Lowering the sintering temperature and enhanced densification by epitaxy in structurally diphasic Al_2O_3 and Al_2O_3–MgO xerogels. Mater Sci Eng 83: 151–159

Tan BH, Jackson I, FitzGerald JD (1997) Shear wave dispersion and attenuation in fine-grained synthetic olivine aggregates: preliminary results. Geophys Res Lett 24(9): 1055–1058

Yeager KE, Burlitch JM (1991) Magnesium methoxide derived catalysis of transesterification, hydrolysis, and condensation of $Si(OMe)_4$ in the sol-gel synthesis of magnesium silicates. Chem Mater 3(3): 387–389

Yeager KE, Burlitch JM, Loehr TM (1993) Intermediates in the sol-gel synthesis of forsterite. Chem Mater 5: 525–534

Yoldas BE (1988) Molecular and microstructural effects of condensation reactions in alkoxide-based alumina systems. In: Mackenzie JD, Ulrich DR (eds) Ultrastructure processing of advanced ceramics. Wiley, New York

Young AC, Lin JC, Yeh TS, Cherng CL (1993) Characteristics of tape casting slurries containing forsterite, PVB and organic solvent. Mater Chem Phys 34: 147–153